International Atomic Energy Agency

INDC(CCP)-332
Distr.: L

INDC INTERNATIONAL NUCLEAR DATA COMMITTEE

TRANSLATION OF SELECTED PAPERS
PUBLISHED IN YADERNYE KONSTANTY (NUCLEAR CONSTANTS 1, 1990)

(Original Report in Russian was distributed
as INDC(CCP)-318/G)

Translated by A. Lorenz
for the
International Atomic Energy Agency

June 1991

INDC(CCP)-332
Distr.: L

TRANSLATION OF SELECTED PAPERS
PUBLISHED IN YADERNYE KONSTANTY (NUCLEAR CONSTANTS 1, 1990)

(Original Report in Russian was distributed
as INDC(CCP)-318/G)

Translated by A. Lorenz
for the
International Atomic Energy Agency

June 1991

Reproduced by the IAEA in Austria
August 1991

91-03120

Contents

ISOTONIC AND ISOTOPIC DEPENDENCE OF THE RADIATIVE NEUTRON CAPTURE CROSS-SECTION ON THE NEUTRON EXCESS

Yu. N. Trofimov
V.G. Khlopin Radium Institute, Leningrad

Abstract

The radiative neutron capture cross-section of nuclei has been derived as a function of neutron excess on the basis of the exponential dependence of the cross-section on the reaction energy. It is shown that unknown cross-sections of stable and radioactive nuclei may be evaluated by using the isotonic and isotopic dependence together with available reference cross-section measurements.

Data on fast neutron radiative capture (P3) cross-sections for medium and heavy mass nuclei are at the present time fragmentary and in some cases highly contradictory. This is particularly true of ^{238}U [1] where the error of the evaluated cross-section is 50%. The present study is a sequel to the work initiated earlier [2] on the systematic dependence of the P3 neutron cross-section on the isotope mass number, $\sigma_{n,\gamma}(A)$. On the basis of the systematics of the P3 neutron cross-sections it is possible:

- to reject contradictory or questionable data, and
- to predict cross-section values of nuclei which are difficult to measure, including those nuclei which are radioactive.

On the basis of the evaluation of P3 neutron cross-sections for nuclei of given parity (three parity groups are taken into consideration here: N and Z even-even, even-odd and odd-even nuclei), the isotopic and isotonic dependence of the cross-section can be represented by

$$\sigma_{\alpha} = \kappa_1 \exp(-\kappa_2 \alpha) \qquad (1)$$

where σ - is the P3 neutron cross-section,
$\alpha=(N-Z)/A$ - is the relative neutron excess parameter,
$k_{1,2}$ - are constants whose values are different for the isotopic and isotonic dependencies, and
A,Z,N - are the number of protons and neutron in the nucleus.

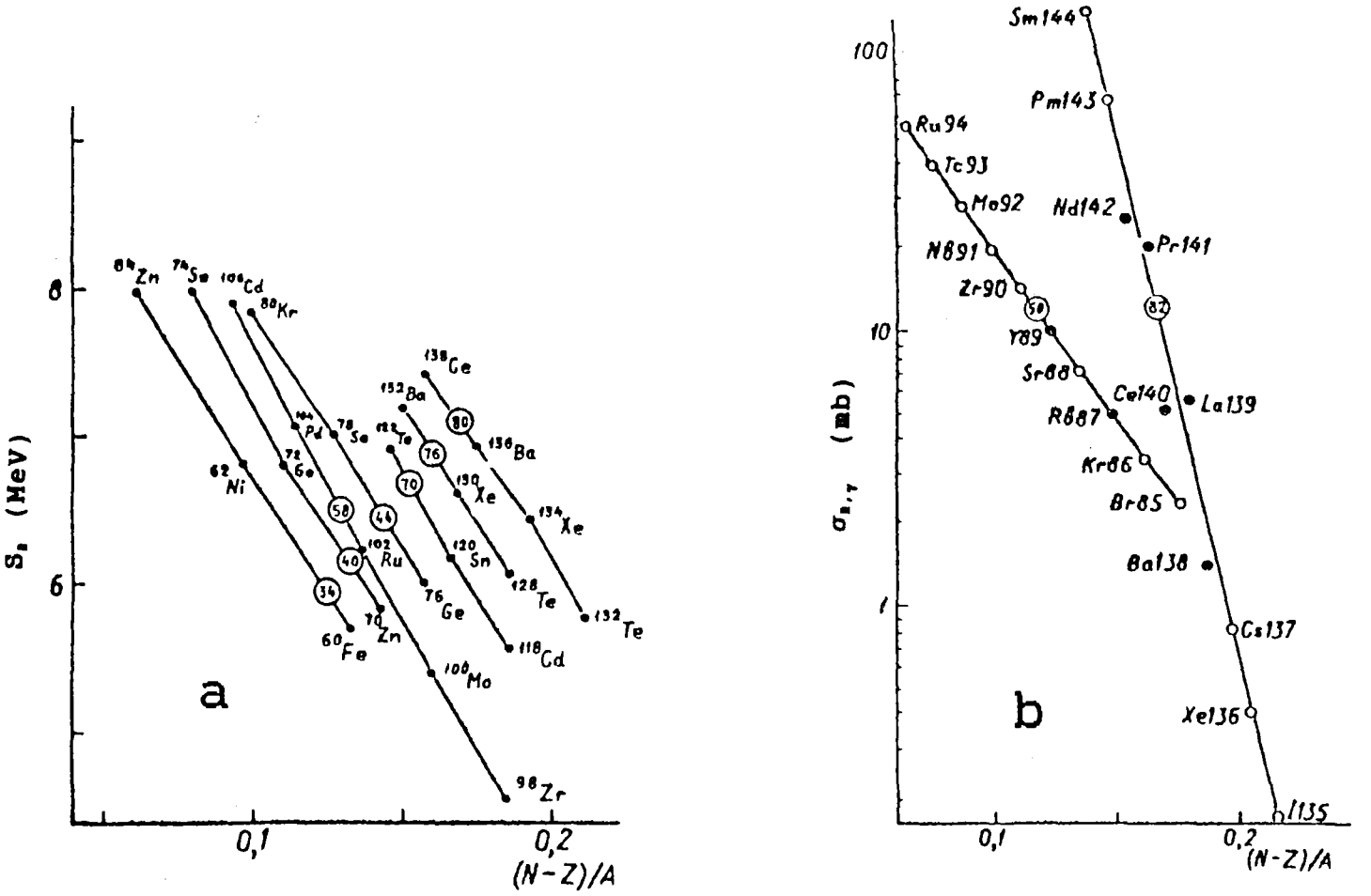

Fig. 1.

Dependence of the target nucleus neutron binding energy on the neutron excess parameter $\alpha=(N-Z)/A$.

For even-even nuclei: points belonging to individual isotones connected by lines are identified by the symbol of the element, the mass number and the neutron number (given in the circles).

a) Non-magic nuclei, N=34,40,58,44,70,80.
b) Magic nuclei, N=50,82.

These dependencies can be substantiated on the basis of the following expression, derived from the evaporation approximation of the statistical theory [3]:

$$\sigma = \kappa_1 \sigma_0 \exp[\kappa_2 (Q - \kappa_3 B)] \qquad (2)$$

where σ, Q - are the cross-section and the reaction energy,
σ_0 - is the geometric cross-section of the nucleus,
B - the Coulomb barrier of the nucleus, and
$k_{1,2}$ - are constants.

Applying equation (2) to the P3 reaction, one obtains

$$\sigma = \kappa_3 \cdot \sigma_0 \exp(\kappa_2 S_n) \qquad (3)$$

where S_n - is the target nucleus neutron binding energy.

If one assumes a linear dependence of S_n as a function of α for an most stable and radioactive isotopes, then equation (3) takes the form of equation (1) for all isotopes (see Fig. 1a).

For magic number nuclei (N=50,82,126), as well as for nuclei which undergo a shape transformation, the linear decrease dependence of $S_n(\alpha)$ does not hold true. In those cases, the isotopic dependence determines only the upper limit of the P3 neutron cross-section. For magic number isotones, the linear decrease behavior of $S_n(\alpha)$ is observed and the isotonic dependence can therefore be used for the evaluation of P3 neutron cross-sections of exotic nuclei (Fig. 1b).

The results of a simultaneous use of the isotopic and isotonic dependencies for the evaluation of the P3 neutron cross-sections at 0.5 MeV for even-even isotopes having N=38,40,52-58,72-78, are shown as an example in Fig. 2, where the complete set of experimental and evaluated data, presented in the form of isotopic (continuous line) and isotonic (broken line) dependencies, is plotted as a function of the neutron excess.

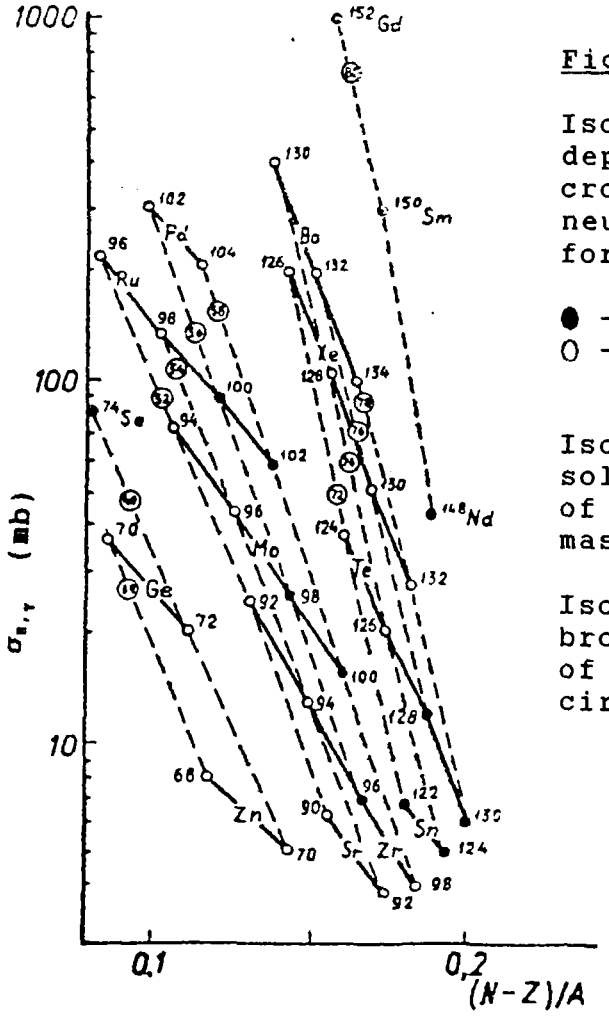

Fig. 2.

Isotopic and isotonic dependence of the P3 neutron cross-section at 0.5 MeV on the neutron excess parameter (n-Z)/A for even-even nuclei:

● - reference data [4],
O - this evaluation by the author

Isotopic dependence given by solid line with identification of element symbol and isotope mass number.

Isotonic dependence given by broken line with identification of the neutron number given in circle.

The position of the straight line which shows the isotopic or isotonic dependence can be determined from known cross-section values for two or more isotopes (isotones), using the cross-section of an isotope and the slope of the line which can be determined by analogy from the slope of the lines for neighboring Z nuclei.

Reference reaction data [4] for the ^{74}Se, ^{96}Zr, ^{98,100}Mo, ^{100,102}Ru, ^{122,124}Sn, ^{128,130}Te, ^{148}Nd, ^{150}Sm, ^{152}Gd isotopes, as well as our evaluated data for the ^{68,70}Zn, ^{70,72}Ge, ^{90,92}Sr, ^{92,94,98}Zr, ^{94,95}Mo, ^{96,98}Ru, ^{102,104}Pd, ^{124,126}Te, ^{126,128,130,132}Xe and ^{130,132,134}Ba isotopes, for which there are no data at the present time, are shown in Fig.2.

In spite of the apparent similarity of the isotopic and isotonic dependencies, there are significant differences. The isotopic dependence provides information on the cross-sections for one and the same element. On the other hand, the isotonic dependence is is derived from information on isotopes of different elements.

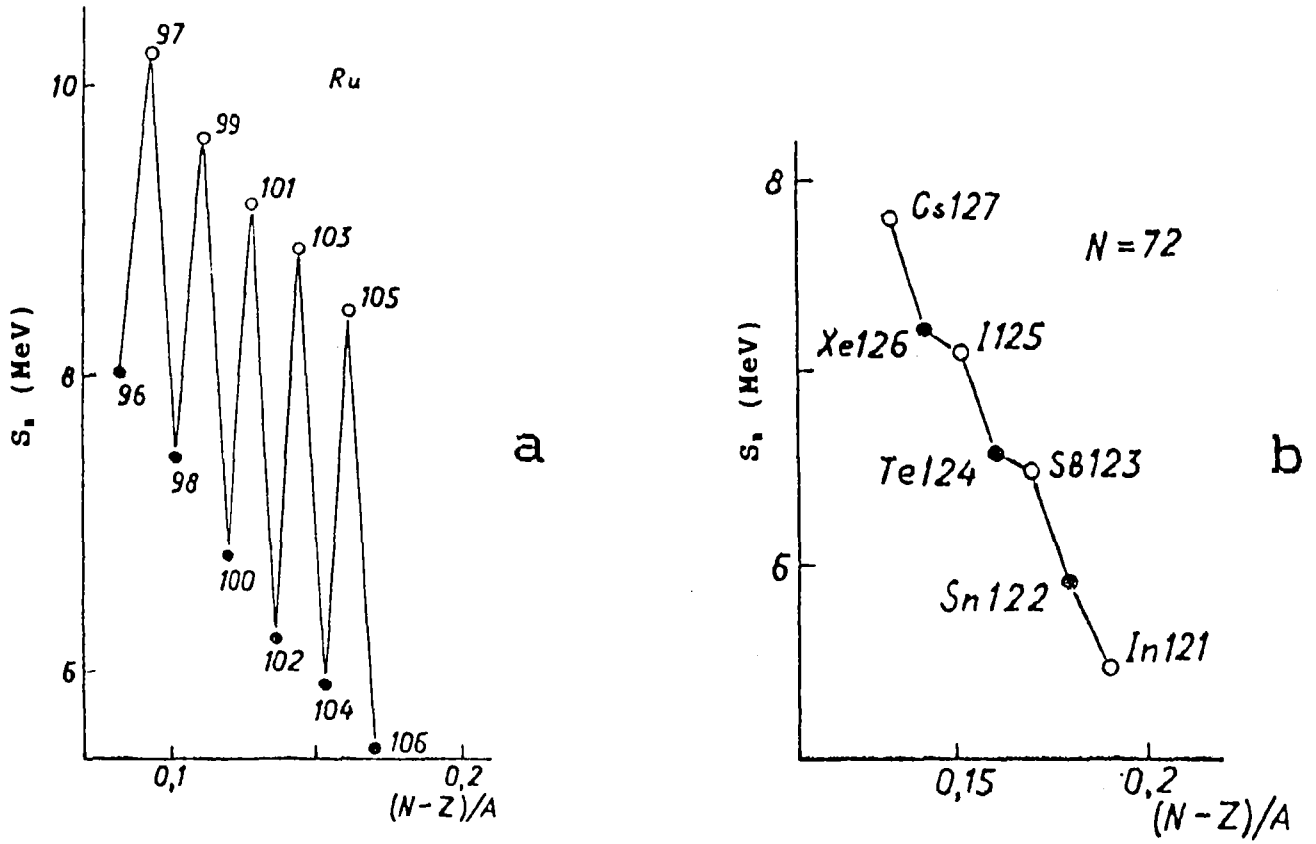

Fig. 3.

Dependence of the neutron binding energy on the neutron excess parameter:

a) Ruthenium isotopes: O - odd neutron number, ● - even neutron number.

b) Isotonic nuclei having a neutron number of 72: O - odd proton number, ● - even proton number.

As a result of this difference it is possible to obtain cross-section values for isotopes of elements which were not part of the initial investigation. Because of the steep slope of the isotonic dependence, this dependence is highly sensitive to changes of the neutron excess parameter. Also, as illustrated in Figs. 3a and b, in the case of the isotopic dependence, the variation of the neutron binding energy as a function of the parity of the number of neutrons in the nucleus is of the order of 2 MeV; in the case of the isotonic dependence, on the other hand, the same variation as a function of the number of protons in the nucleus is an order of magnitude smaller (i.e., 0.1 to 0.3 MeV). For magic nuclei (for neighboring Z values) having N values of 50 and 82, the neutron binding energy is practically independent of the proton number parity.

The various aspects of these dependencies makes it possible to perform cross-section evaluations for a wider number of isotopes, and allows one to utilize a larger number of reference nuclei in these evaluations.

REFERENCES

[1] BULEEVA, N.N., et al., Atomnaya Ehnergiya 5 (1988) 348 (in Russian).

[2] TROFIMOV, Yu.N., Proc. All-Union Conf. on the "Production and utilization of isotopes and of nuclear radiation sources in the USSR industry", Leningrad 1988, TsNIIatominform, Moscow (1988) 27 (in Russian).

[3] TROFIMOV, Yu.N., Problems of Atomic Science and Technology. Ser. Nuclear Constants 2 (1979) 47 (in Russian).

[4] BELANOVA, T.S., et al., Neutron Radiative Capture Ehnergoatomizdat (1986).

INVESTIGATION OF THE $^{10}B(n,t)$ REACTION CROSS-SECTION IN THE SUBTHRESHOLD ENERGY REGION

N.V. Kornilov, A.V. Balitskij, V.Ya. Baryba, V.I. Druzhnin,
A.B. Kagalenko, A.K. Kharitonov
Institute of Physics and Power Engineering, Obninsk

Abstract

The $^{10}B(n,t)$ reaction cross-section has been measured at incident neutron energies of 0.025 eV, 420 keV and 5 MeV. A detailed description of the experimental technique and the Monte Carlo simulation is given. It was confirmed that the cross-section of this reaction in the subthreshold region is non-zero. The recommended value of the $^{10}B(n,t)$ reaction cross-section at thermal is 8.5±2.0 mb.

Introduction

The importance of the investigation of the $^{10}B(n,t)$ process is due to its effect on the radiation environment in nuclear power plants. According to the data published in references [1,2] the $^{10}B(n,t)$ reaction is the principal, or one of the principal sources of tritium resulting from reactor operation.

In our work reported in reference [3], the $^{10}B(n,t)$ reaction cross-section was evaluated in the 1.5 to 20 MeV region. On the basis of the existing experimental data, it could be inferred that the accuracy of the cross-section in the 2.5 to 10 MeV energy interval was ≈15%, and ≈20% in the 10 to 20 MeV energy range. Until now, this reaction cross-section has not been investigated below 2.5 MeV. The present investigation was stimulated by the need for a measurement of this reaction cross-section in that energy range, including a measurement at thermal.

Irradiation of the Samples

The $^{10}B(n,t)$ reaction cross-section was measured by activation. Two samples were irradiated at each measurement energy, one to record the background only, and one to record the background plus the effect of the reaction so as to take into account the contribution of the room return neutrons to the total tritium

production, and as a check to ascertain whether any extraneous tritium, which may have been present in the room, penetrated into the sample. The irradiation of each sample lasted 60 to 100 hours.

a) E_n= 0.025 eV. The irradiation at this energy was performed in the thermal column of the BR-10 reactor. The irradiated sample "sandwich" (consisting of the sample and the monitor foils) was located in the center of the T-4 channel, and the background detection sample was put to the side and behind the shielding. The $^{197}Au(n,\gamma)$ reaction was used to monitor the neutron flux; the thermal flux, measured in the T-4 channel was (2.2×10^8) n/s·cm^2.

b) E_n= 420 keV. Monoenergetic 420 keV neutrons were obtained from the T(p,n) source reaction using the KG-2.5 accelerator. The "sandwich" sample was secured to the body of an ionization fission chamber, which served to monitor the variation of the neutron flux with time. The sample was placed 2.5 cm from the target. The $^{235}U(n,f)$ reaction was used as the monitor reaction. For an average accelerator current of ≈30 mA, the neutron flux incident on the sample was (4.4×10^7) n/s·cm^2.

c) E_n= 5MeV. The D(d,n) reaction was used as the source of 5 MeV neutrons. The irradiation geometry was the same as for the 420 keV irradiation. The $^{58}Ni(n,p)$ reaction was used as the monitor reaction. A correction was made to account for the possible generation of ^{58}Co, both in the ground state as well as in the isomeric state. For an average accelerator current of ≈30 mA, the neutron flux incident on the sample was (2.6×10^7) n/s·cm^2. The measurement performed at this energy served to check the methodology of the experiment.

The relative magnitude and energy spectrum of the neutron flux incident on the sample and on each of the monitor foils, for the actual irradiation geometry and taking the kinematics of the reaction in the target into account, were calculated using the Monte Carlo method for the two cases described in b) and c) above. (See reference [4] for details).

Detection of the Tritium

The following methods have been used until now to measure the $^{10}B(n,t)$ reaction cross-section:

a) by counting the actual ("triple star") $^{10}B(n,t)$ events in borated photoemulsions [5], or by measuring the peak of the event amplitude distribution in boron-containing proportional counters [6,7], and

b) by counting the tritium reaction product or the subsequent ^{3}He β-decay product after their separation from the sample [8-13].

A detailed analysis of experiments which have been conducted until 1987 is given in reference [3]. It must be noted at this point that the detection of $^{10}B(n,t)$ decay events presupposes the use of samples spiked with very small quantities of boron (in counters or emulsions), requiring consequently very large integral neutron fluxes. In order to detect the T or the ^{3}He reaction products one could increase the mass of the sample up to a few grams, and consequently manage with a lower integral flux; however, the extraction of the reaction products is coupled with significant technical difficulties.

In our experiment we succeeded in developing a technique which allowed us to use a relatively large amount of boron (0.05 to 0.1 g), and avoid at the same time the reaction product extraction procedures. The sample consisted of a boron-bearing scintillator hermetically encapsulated in a quartz housing. The samples were irradiated in monoenergetic neutron fluxes. The amount of tritium generated in the sample during the irradiation period was determined by registering the scintillation events induced by the β-particles emitted by the tritium within the sample.

The samples were composed of the ZhS-1 scintillator compound containing 32% methyl borate (trimethyl ethyl borate). On the basis of a 92% enrichment of ^{10}B, the ZhS-1 methyl borate mixture contained 3.022% by weight of ^{10}B.

Although an increase of the ^{10}B content in the samples, by adding methyl borate to the scintillator, would increase the number of

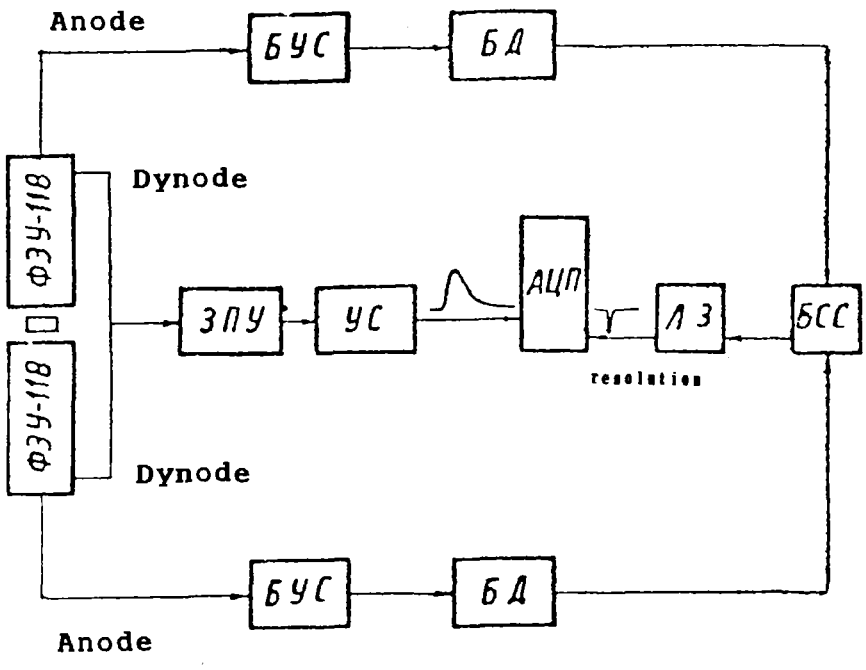

Fig. 1. Block diagram of the assembly for the measurement of the activity of irradiated samples. Spectrometer channel: the total signal from the ФЭУ-118 photomultiplier dynode, proportional to the brightness of the light pulse, is transmitted through the preamplifier ЗПУ and the amplifier УС, to the АЦП circuit. Time channel: the amplified anode signal is transmitted to the fast discriminator БД. Only those signals are counted which are recorded by the fast coincidence circuit БСС within a time window of $\tau=\pm 15$ns.

^{11}B atoms in the samples, it would at the same time lower the scintillation intensity as well as the tritium β- decay detection efficiency. The percent content of methyl borate is practically inversely proportional to the light emission intensity of the scintillator. The chosen concentration of the methyl borate was such that its light emission intensity corresponded to that of the tritium-bearing compound used in the standard SORTV source.

The low energy limit of the tritium beta decay spectrum (E_{min}=18.61 keV) leads to the situation in which the magnitude of the scintillation event signal is comparable to the level of the internal photomultiplier noise. The method used to separate the scintillation signal from the background noise is based on the fast coincidence technique (see Fig. 1), which selects only those events which fall into a narrow enough time window ($\tau=\pm 15$ ns).

Typical signal amplitude spectra are shown in Fig. 2. Also shown in this figure are spectra calculated by the Monte Carlo method modelled according to the "tritium+scintillator+photomultiplier +electronics" stages of the experiment.

These model calculations were performed (a) in order to confirm that the observed amplitude spectrum is indeed the tritium beta decay spectrum, and (b) to establish the relationship between the efficiency of beta decay event detection and the light emission of the sample.

The following was assumed in the modelling of the scintillation event amplitude spectrum generated by the beta decay of the tritium:

1 - the energies of the tritium beta decay particles have a Fermi distribution [14],

2 - the scintillation event intensity (i.e., the average number of photoelectrons μ) is a function of the energy of the beta decay particle E_β,

3 - the number of the photoelectrons N, generated by a beta particle of energy E_β, have a Poisson distribution with an average value of $\mu(E_\beta)$,

4 - the probability that M photoelectrons were recorded in the first photomultiplier, and that (N-M) were recorded in the second, has a binomial distribution,

5 - the fluctuation in the number of secondary electrons in the photomultiplier has a normal distribution, and

6 - only those decay events were counted, whose signal from each of the photomultipliers was higher then the corresponding counting threshold (i.e., only coincident pulses were counted).

The calculations were performed on the assumption that the dependence of the average number of photoelectrons on the beta particle energy could be either linear ($\mu(E)=const \cdot E_\beta$) or non-linear (see references [15] and [19]).

The determination of the unknown parameters, namely the absolute number of photoelectrons for a given beta particle energy (i.e., the values of the "const" coefficient in the linear, or the corresponding coefficient in the non-linear dependence) and the

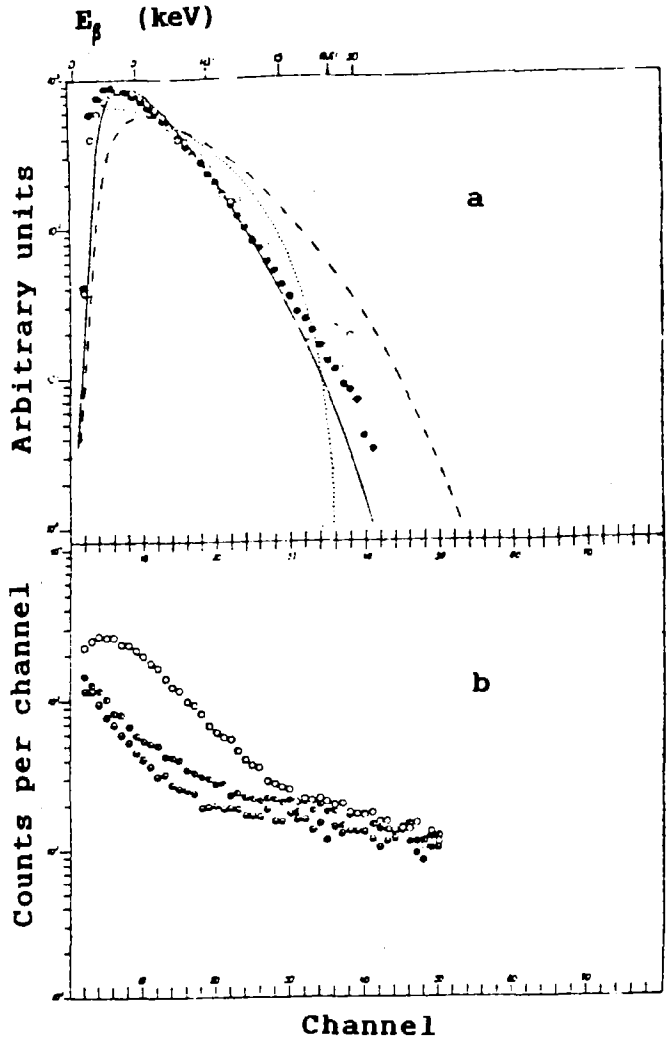

Fig. 2 . Experimental and calculated pulse spectra:

a) ● - SORTV standard source spectrum,
O - measured irradiated sample spectrum,
------ linear dependence calculation,
———— non-linear dependence calculation,
The Fermi energy spectrum for tritium β particle decay is given by the dotted line on the upper scale.

b) measured pulse spectra (10000 s measurement time)
◒ - without scintillating sample,
● - with an un-irradiated sample,
O - with irradiated scintillating sample.

amplification coefficient for the "photomultiplier+electronics" stage, was done by calculating the peak shape in the amplitude spectrum when the scintillator is irradiated with ^{241}Am ≈60 keV gamma rays; both of these parameters, the "const" and the amplification coefficient, were determined by comparing the calculated values with the experimental values of the distribution and of the location of the peak in the amplitude

distribution, respectively. The value of the last unknown parameter, the "counting threshold", was chosen so that only single electron pulses were counted. This set of parameters was then used in calculating amplitude spectra generated by the beta decay of tritium.

It can be seen in Fig. 2 that the spectrum calculated on the assumption of a linear dependence of μ on E_i differs sharply from the measured spectrum; it was therefore decided to use the energy dependence $\mu(E_i)$ which had been measured in the experiments described in references [15] and [16] normalized to the absolute value described above. The dependence $\mu(E_i)$, calculated in this manner, agreed very well with the measured spectrum, which allowed us to use this model with confidence.

In order to determine the total amount of tritium generated in the sample, it was necessary to know the dependence of the recording efficiency ε of our experimental assembly for a given light pulse magnitude x, which is slightly different from the light emission of the standard used for the tritium-bearing source SORTV with a given activity (the light emission differs from one sample to another by approximately 10%, and they differ from the SORTV light emission standard by 10%-15%).

The calculated $\varepsilon(x)$ function is in good agreement with the experimentally determined $\tilde{\varepsilon}(x)$ dependence, including the effect of different degrees of darkening of the SORTV source:

$$\varepsilon(x) = \varepsilon_0 [1 + (x-1) \cdot 0.83]$$
$$\tilde{\varepsilon}(x) = \varepsilon_0 [1 + (x-1) \cdot 0.77]$$

where x = (sample light emission)/(SORTV light emission)
and $\varepsilon_0 = 0.4$.

In order to reduce the intensity of the gamma ray background, the recording part of the experimental assembly was surrounded by lead shielding. This also helped reduce the intrinsic noise level of the detector assembly to ≈ 1.5 imp./s in the energy range of 1-20 keV.

The background noise of the experimental assembly consisted of:

1) random coincidences (0.1-0.3) /s in the amplitude range covered by channels 0 to 4,

2) actual coincidences recorded without any scintillating sample, and

3) background due to the interaction of gamma rays with the scintillator (see Fig. 2)

Consequently, the following measurements were repeated a number of times for each individual i^{th} sample: beta-particle spectrum from the irradiated sample N_c, spectra from non-irradiated samples N_i, and spectra without sample N_0. The actual effect was determined after the subtraction of the background due to random coincidences using the following expression:

$$N_i^{eff} = N_i - \frac{M_i}{M_c} (N_C - N_O)$$

where M_i and M_c are the masses of the irradiated and non-irradiated i^{th} scintillator, respectively. The signal to noise ratio varied as a function of the amount of generated tritium from ≈0.1 at thermal energy to ≈4 for E_n=5 MeV.

Discussion of Results

The results of this investigation are summarized in the Table below. The activity of the tritium in the irradiated samples and the statistical uncertainty of their measurement are listed in the second column. The reaction cross-section and its errors is given in the fourth column. The following error components were taken into consideration:

1) the accuracy of the activity determination,

2) the accuracy in the determination of the neutron flux, which is ≈5% at E_n=5 MeV and ≈20% for E_n=420 keV and 0.025 eV,

3) the accuracy in the determination of the tritium counting efficiency, which is estimated at ≈5%.

The activity of the sample which had been irradiated at a distance of ≈1m from the target is given in the bottom row of the table. Although the agreement shown between two successive measurements at a neutron energy of 5 MeV, illustrates the good

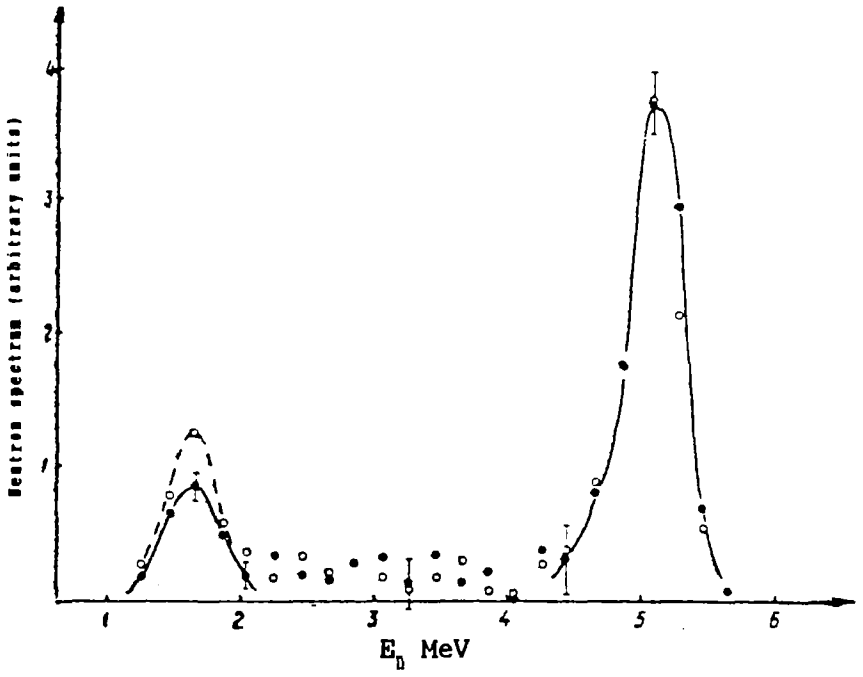

Fig. 3. Neutron spectrum from a solid TD target irradiated by 2 MeV deuterons:

● - at the start of irradiation,
O - after an irradiation time of 20 h and an average beam current of 30 μA

The solid deuteron target has a 1.5 mg/cm^2 layer of titanium on a copper substrate.

reproducibility of the results, the cross-section measured at a neutron energy of 5 MeV is systematically lower than the value recommended in reference [3]. There could be a number of reasons for such a discrepancy.

Thus, it is possible that the neutron spectrum emitted by the target can change in the course of its irradiation as a result of deuteron build-up in the base of the solid deuterium target, giving rise to additional neutrons with energies ranging from 3 to 5 MeV. There is also the possibility of a noticeable reduction in the yield of the basic neutron group. These factors could cause a general decrease of the average neutron energy, in the course of a lengthy irradiation time, to a value that is noticeably lower than 5 MeV. Measurements made with a single crystal spectrometer have shown an absence of neutrons generated by a so-called "built-up" target (see Fig. 3). During an irradiation of ≈20 hours, the yield of 5 MeV neutrons did not drop by more than 5% to 10%. Neutrons with energies of

approximately 1.5 MeV, which are generated by the $^{12}C(\alpha,n)$ reaction (as a result of a deposition of carbon on the surface of the target in the process of its preparation and use) cannot be expected to contribute an input from the $^{10}B(n,t)$ and $^{56}Ni(n,p)$ reactions to any noticeable degree, and are therefore of no consequence to the considerations of this experiment.

RESULTS OF THE $^{10}B(n,t)$ REACTION CROSS-SECTION MEASUREMENTS

(1)	(2)	(3)	(4)	(5)	(6)
0.025 eV	0.23±0.16	$^{197}Au(n,\gamma)$	4.7±3.4	6.0±4.0	12.5±2.5 [12]
	-	-	-	-	7.0±2.0 [7]
	-	-	-	-	50.0±6.0 [11]
420 keV	0.47±0.20	$^{235}U(n,f)$	5.0±2.4	7.0±3.0	-
5.0 MeV	4.58±0.20	$^{58}Ni(n,p)$	163±14	217	217 [3]
	6.46±0.20	$^{58}Ni(n,p)$	163±14	-	-
5.0 MeV Background	-0.02±0.20	-	-	-	-

(1) Neutron energy
(2) Tritium activity 1/s
(3) Monitor reaction
(4) $\sigma\pm\Delta\sigma$ (measured)
(5) $\sigma\pm\Delta\sigma$ (normalized)
(6) Other measurements

Another reason for this discrepancy could be attributed to the leakage of the tritium from the scintillator to the photomultiplier, which could reduce the measured activity. There is also the possibility that the enrichment of the ^{10}B in the methyl borate could be different than the used value of 92%.

However, since all of these effects were the same for all of the irradiations, the measured cross-sections were normalized to the recommended value at 5 Mev given in reference [3]. The results, thus renormalized, are listed in the fifth column of the Table.

As can be seen, the cross-section of the $^{10}B(n,t)$ reaction at thermal falls within the limits of the uncertainties of the data published in 1987 and 1988. The average value of the cross-section, taking into account the result of this experiment and those reported in references [7] and [12] is (8.5±2.0) mb, which is substantially lower than the value given in reference [11].

It can therefore be concluded that the value of the $^{10}B(n,t)$ reaction cross-section at thermal is known at the present time to an accuracy of 20%. In spite of the technical difficulties encountered in the measurement of low cross-sections, a reasonable agreement has been achieved between measurements using different experimental methods.

REFERENCES

[1] BADAYEV, V.V., EGOROV, Yu.A., SKLYAROV, V.P., Radiation Safety and Protection 0f Nuclear Power Plants, Moscow (1981) 64 (in Russian).

[2] SHAGALIN, N.M., INYUTIN, E.I., OTSTAVNOV, P.S., "Formation and transfer of tritium in fast reactors", Franco-Soviet Seminar on Fast Reactor Safety Concepts, Obninsk (1981) (in Russian).

[3] KORNILOV, N.V., KAGALENKO, A.B., DAROTSI, Sh., TCHERPAK, F., in Proc. First International Conference on Neutron Physics, TSNIIatominform, Moscow, Vol.3 (1988) 163 (in Russian).

[4] KORNILOV, N.V., Proc. Advisory Group Meeting on the Properties of Neutron Sources, Leningrad 1988, IAEA-TECDOC-410 (1989) 320.

[5] FRYE, G.M., GAMMEL, J.H., Phys. Rev. 103 (1956) 328.

[6] DAVIS, E.V., GABBARD, F., BONNER, T.W., BASS, R., Nucl. Phys. 27 (1961) 448.

[7] KAVANAGH, W., MARCLEY, R.G., Phys. Rev. C36 (1987) 1194.

[8] WIMAN, M.E., FRYER, E.M., THORPE, M.M., Phys. Rev. 112 (1958) 1264.

[9] SUHAIMI, A., WOLFE, R., QAIM, S.M., STOCKLIN, G., Radiochimica Acta 40 (1986) 113.

[10] BOEDY, Z.T., MIHALI, K., Compilation and Evaluation of (n,t) Cross-Sections around 14 MeV, IAEA Rep. INDC(HUN)-22 (1985).

[11] CSERPAK, F., BIRO, T., CSIKAI, J., Proc. Int. Conf. on Neutron Physics and other Applications, Harwell (1978) 761.

[12] QAIM, S.M., et al., Proc. Int. Conf. on Nuclear Data for Science and Technology, Mito, Japan (1988) 225.

[13] QAIM, S.M., WOLFE, R., Nucl. Phys. A295 (1978) 150.

[14] FERMI, E., Z. fuer Phys. 88 (1934) 161.

[15] TAYLOR, C.J., et al., Phys. Rev. 84 (1951) 1034.

[16] SCHMELING, H-H., Z. fuer Phys. 160 (1960) 520.

EXPERIMENTAL AND CALCULATIONAL STUDIES OF THE TRANSMISSION OF FISSION SPECTRUM NEUTRONS THROUGH Cr AND Ni SPHERES

O.V. Baranov, V.V. Korobeinikov, V.M. Lityaev,
A.M. Tsibulya, V. Hansen, V. Vogel
Institute of Physics and Power Engineering, Obninsk,
Central Institute for Nuclear Research, Rossendorf, GDR.

Abstract

Results of the analysis of neutron transmission through Cr and Ni spheres are given. The experiments have been carried out in the USSR and in the GDR. The experimental transmission functions determined in the USSR are in good agreement with the neutron leakage spectra studied in the GDR experiments.

Introduction

The formulation and checking of group cross-section data used in reactor and shielding calculations is usually based on integral experiments. One of the more significant integral experiment is the study of the ^{238}U removal cross-section below the fission threshold. Characteristics of fast reactors, such as k_{eff} and the breeding ratio, can be calculated with the aid of the BNAB [1] group cross-section data library to an accuracy of 1.4% and 2.4%, respectively. A significant fraction of these errors (0.8% and 1.2% respectively) is due to the uncertainty in the value of the removal cross-sections of ^{238}U below the fission threshold as well as those of construction materials. Although this reaction has been studied in sphere transmission experiments in our country as well as in the West in the 1950's, it was pointed out in the world request list for nuclear data, WRENDA [2], that this uncertainty could be reduced by repeating these sphere transmission experiments using improved contemporary technology. As a result of these considerations, these experiments were performed in our country and in the GDR.

Experimental Set-up and Measurement Method

Neutron transmission experiments were performed at the USSR Institute of Physics and Power Engineering (FEI), in a modified

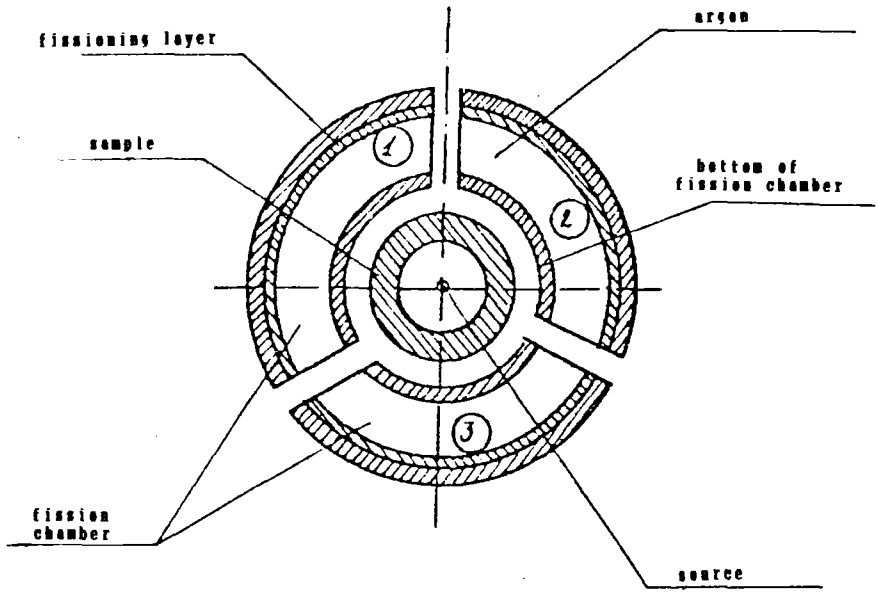

Fig. 1 Diagram of experimental assembly 1

spherical geometry. The neutron source consisted of a vial with ^{252}Cf placed at the centre of the sphere being measured. Three fission chambers were placed up against the spherical shell sample within the sphere. The inner surface of the outer shell of the sphere was lined with a layer of 99.99% isotopically pure ^{238}U, with a thickness of ≈ 1 mg/cm^2; this insured a good counting efficiency of the fission chambers and guaranteed good reproduceability of the results. Each chamber was in the form of a spherical segment which encompassed a solid angle of $\approx 0.6\pi$. The angles between the centres of each two chambers was 120^0, and the total solid angle encompassed by all three chambers was close to 2π. The geometry of the experimental assembly is shown in Fig. 1. The distance between the surface of the sample and the chamber electrodes coated with the layer of ^{238}U was 5 mm. This quasi-spherical geometry reduced the noise-to-signal ratio considerably.

The neutron transmission experiments were conducted with spherical samples of nickel and chrome. The nickel sample consisted of an all-metallic spherical shell; the chrome sample consisted of chrome powder packed into a container made of copper in the shape of a spherical shell.

One of the results of the first series of experiments was the ratio:

$$T(t) = \frac{N(t)}{N_o} \qquad (1)$$

where $N(t)$ - is the detector count with sample of thickness t,
N_0 - is the detector count without sample.

The second series of experiments, conducted in the GDR, consisted of an investigation of the neutron leakage spectrum from the same spherical samples. The arrangement of the experimental assembly is shown in Fig. 2. In the 800 keV to 10 MeV energy range, the neutron spectrum was measured with a stilbene scintillation spectrometer, and in the 40 keV to 1.1 MeV range it was measured with a set of spectrometric proton recoil detectors.

The following two sets of experiments were conducted:

1 - Measurement of the neutron spectrum emitted by the source (without sample), and

2 - Measurements of the neutron leakage spectrum emitted by the investigated material samples.

Experimental and Calculational Results

Characteristics of the spherical samples:

Nickel (99.5%) - outer diameter: 170 mm
- inner diameter: 30 mm.

Chrome (99.8%) - (in the form of a chrome powder filled copper container) - chrome grain size: 0.02 - 0.2 mm.
- outer diameter of copper container: 160 mm,
- outer diameter of the chrome shell: 157.8 mm,
- inner diameter of copper container: 29 mm,
- inner diameter of the chrome shell: 32 mm,
- weight of the copper container: 863.8 g,
- weight of the chrome powder: 9016 g.

The transmission functions were measured at the FEI in the USSR, and the neutron leakage spectra were measured in the GDR.
The experiments were analyzed by the Monte Carlo method, using the MMFK code [3], and by transport calculations in the S_8 approximation using the ROZ-B code [4]. The measured spectrum of neutrons emitted by the ^{252}Cf source (without sample), is shown in

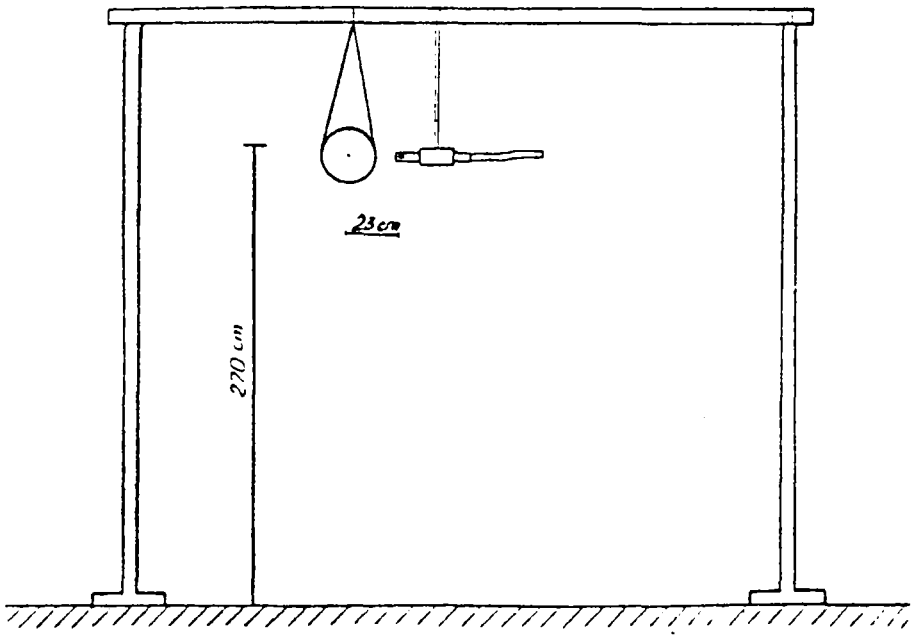

Fig. 2 Diagram of experimental assembly 2

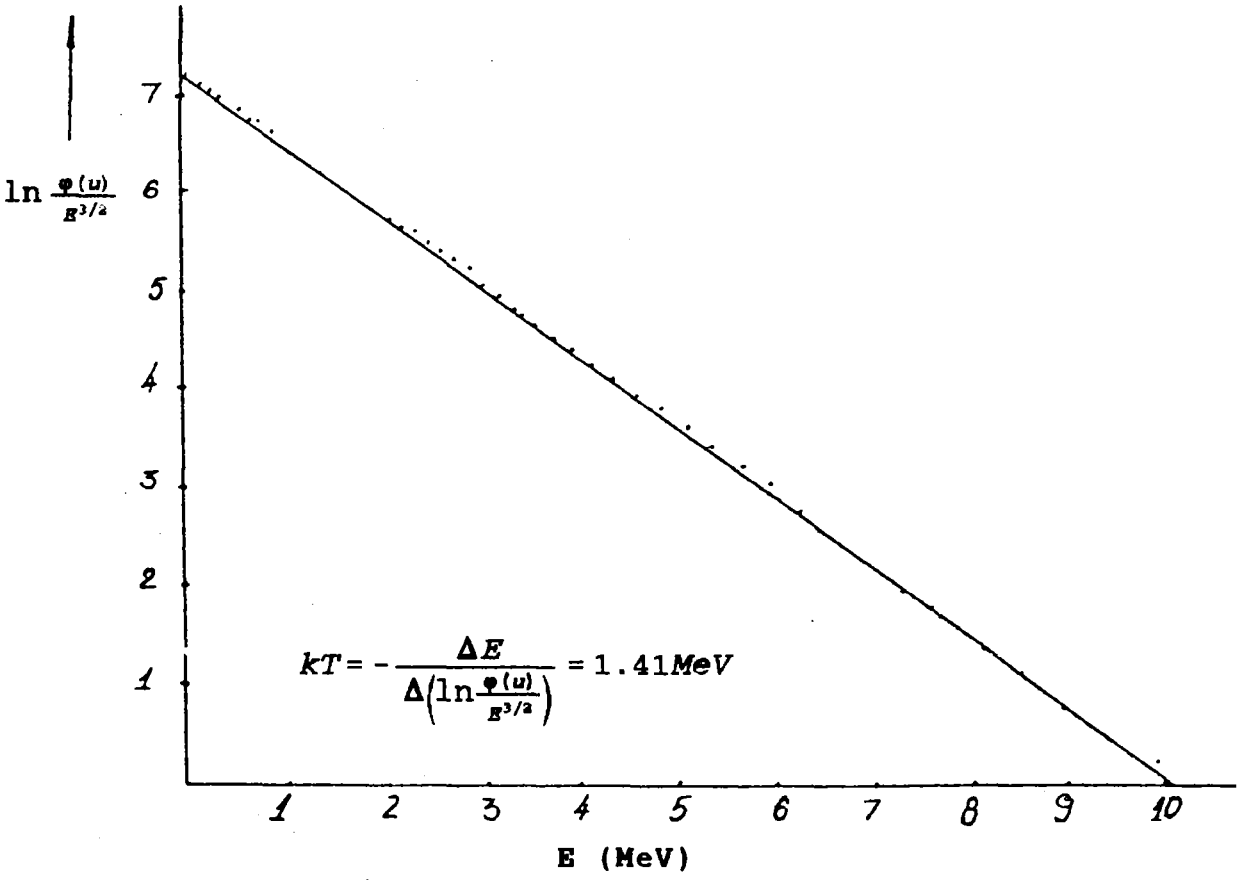

Fig. 3 Measured neutron spectrum

Fig. 3. Using the scale shown on the right, this spectrum can be easily approximated by

$$\ln \frac{\Phi(E)}{E^{1/2}} = \frac{\Phi(u)}{E^{1/2}}$$

a straight line whose slope gives a value of kT = 1.41 MeV, which is in good agreement with the theoretical value.

A comparison between the measured and the calculated neutron leakage spectra from the spherical samples are shown in Figs. 4 and 5. The measured spectra, and the californium source spectrum are given per unit lethargy used in the BNAB group cross-section library. It can be seen from these results that there is good agreement between the calculated and measured neutron leakage spectra in the energy range of 0.8 and 10.5 MeV for both samples.

Figs. 6 and 7 shows the group transmission functions:

$$T_g = \frac{\varphi^g_{ob}}{\varphi^g_{Cf}} \qquad (1a)$$

where φ^g_{ob} - is the neutron flux emitted by the sample, and
φ^g_{Cf} - is the neutron flux emitted by the ^{252}Cf source.

It can be seen from the comparison of the calculational and experimental results of the transmission function that there is good agreement for both samples in the energy range of 0.8 to 10.5 Mev. The measured leakage spectrum uncertainty is approximately 5% above 100 keV and about 10% at lower energies. The difference between the measured and calculated transmission functions is 10% for Ni for energies below 0.8 MeV, and more than 20% in the energy range of 46.4 to 100 keV for Cr. The comparison between measured and calculated leakage spectra for both Ni and Cr (not using the BNAB lethargy scale) are shown in Figs. 8-10. Fig. 9 also shows the leakage spectrum for Ni calculated in a multigroup approximation. It can be seen that the multigroup calculation (using the MULTIK code) depresses the leakage spectrum in the 0.8 to 10.5 MeV energy region in comparison to the measured spectrum and to the one calculated with the BNAB data library.

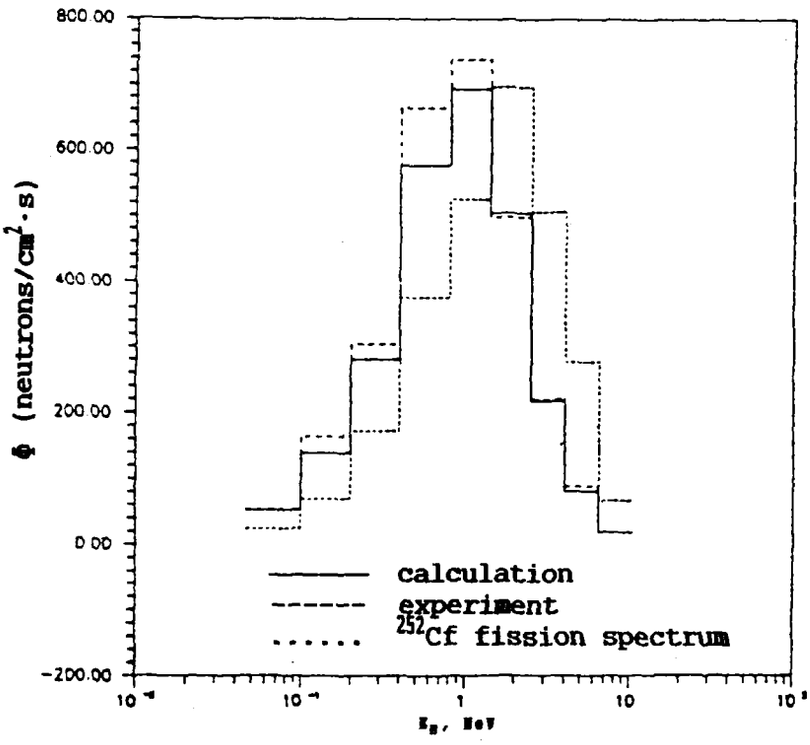

Fig. 4 Group leakage spectrum for Ni sample

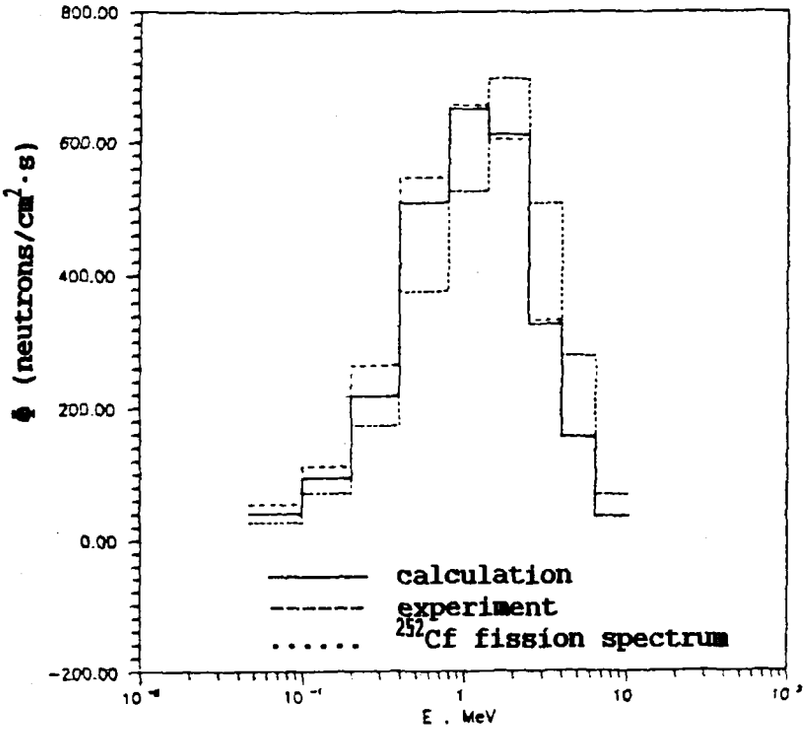

Fig. 5 Group leakage spectrum for Cr sample

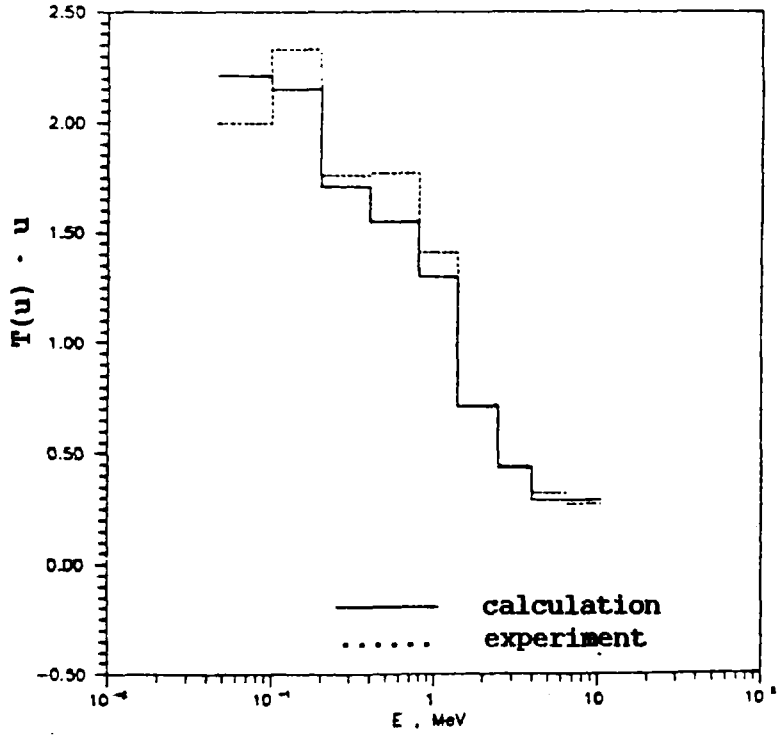

Fig. 6 Group transmission functions for Ni sample

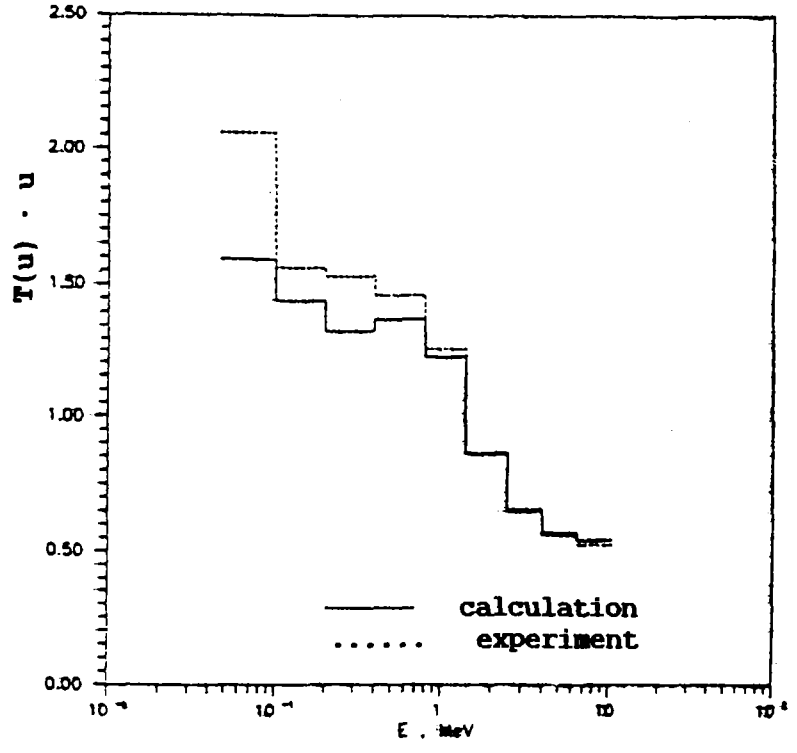

Fig. 7 Group transmission functions for Cr sample

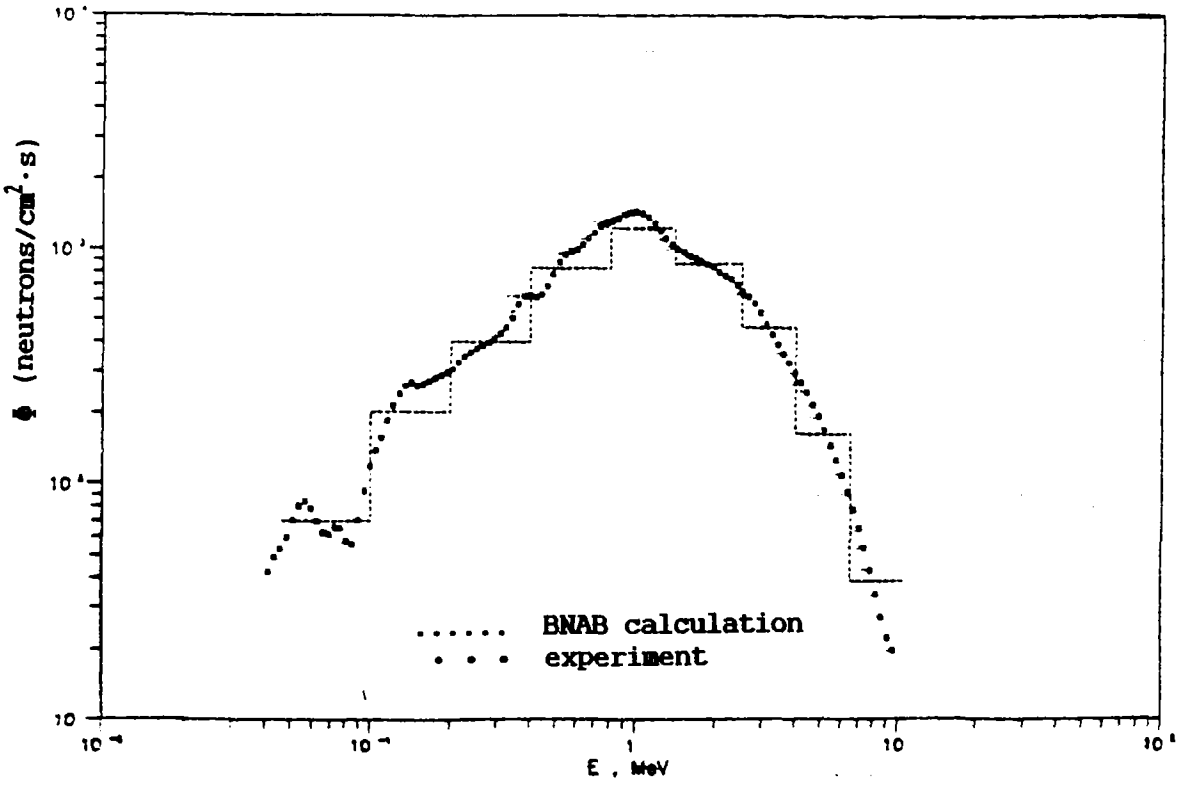

Fig. 8 Leakage spectrum from Ni sphere

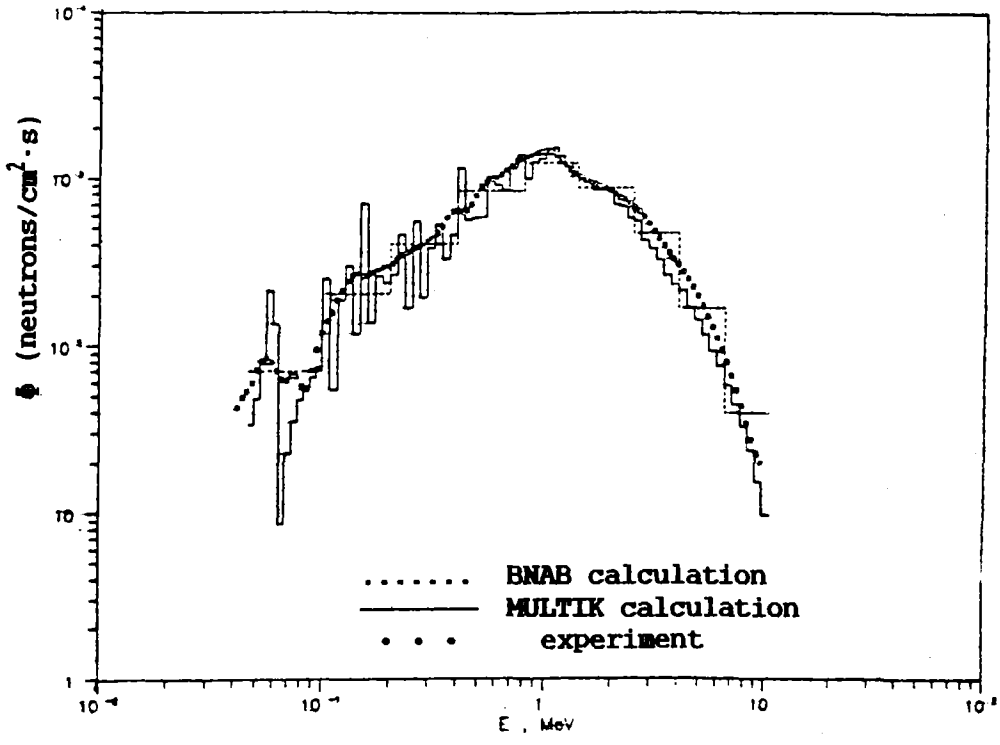

Fig. 9 Leakage spectrum from Ni sphere

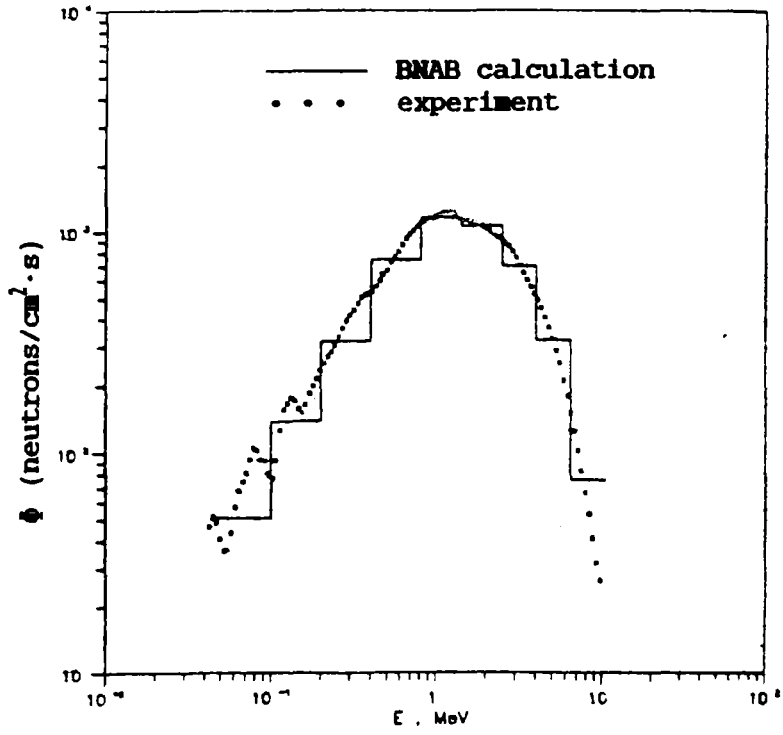

Fig. 10 Leakage spectrum from Cr sphere

COMPARISON OF CALCULATED AND MEASURED TRANSMISSIONS

Sphere		T_t	T_p	σT_p	T_t^∞	T_p^∞
Ni	FEI	0.626±0.002	0.602	1.113	0.562±0.002	0.541
	CINR	-	-	-	0.537±0.03	-
Cr	FEI	0.810±0.002	0.807	1.06	0.761±0.002	0.764
	CINR	-	-	-	0.724±0.04	-

The experimental results obtained at the FEI were adjusted to good geometry conditions. These results, listed in the Table above, show that the transmissions measured by both methods for one of the two materials are in good agreement with each other within the limits of the experimental uncertainty.

Conclusions

The following conclusions can made on the basis of the results of this series of experiments:

1. The Ni removal cross-section derived from the experiments performed in the USSR is lower than the one given in the BNAB data library by 6%.

2. On the basis of the good agreement between the calculated and measured neutron leakage spectra in the 0.8 to 10.5 MeV energy range, it can be assumed that the structure of the inelastic scattering matrix for Ni and Cr is correct in this energy region.

3. Multigroup calculations yield lower values of the neutron leakage spectra in the 0.8 to 10.5 MeV energy range.

4. Further investigation of neutron leakage spectra in the energy region below 0.8 MeV would be of interest to improve the knowledge of the cross-section for the inelastic transport from the upper energy region to the lower energy region.

REFERENCES

[1] ABAGYAN, L.P., BAZAZYANTS, N.O., NIKOLAEV, M.N., TSIBULYA, A.M., Group Constants for Reactor and Shielding Calculations, Ehnergoizdat, Moscow (1981) (in Russian).

[2] INTERNATIONAL ATOMIC ENERGY AGENCY, World Request List for Nuclear Data 1979-1980, Rep. INDC(SEC)-73 (1979).

[3] FRANK-KAMENETSKIJ, A.D., Problems of Atomic Science and Technology, Ser. Physics and Technology of Nuclear Reactors 8 (1981) 16 (in Russian).

[4] VOLOSHCHENKO, A.M., KOSTIN, E.I., PANFILOVA, E.I., UTKIN, V.A., ROZ-B - Set of computer codes to solve the transport equation in one-dimensional geometry: users' manual, IPM Institute Acad. Nauk SSSR, Moscow (1980) (in Russian).